
This is an electronic reprint of the original article.
This reprint may differ from the original in pagination and typographic detail.

Hautojarvi, P.; Huomo, H.; Puska, M.; Vehanen, A.

Vacancy recovery and vacancy-hydrogen interaction in niobium and tantalum studied by positrons

Published in:
Physical Review B

DOI:
[10.1103/PhysRevB.32.4326](https://doi.org/10.1103/PhysRevB.32.4326)

Published: 01/10/1985

Document Version
Publisher's PDF, also known as Version of record

Please cite the original version:
Hautojarvi, P., Huomo, H., Puska, M., & Vehanen, A. (1985). Vacancy recovery and vacancy-hydrogen interaction in niobium and tantalum studied by positrons. *Physical Review B*, 32(7), 4326-4331.
<https://doi.org/10.1103/PhysRevB.32.4326>

This material is protected by copyright and other intellectual property rights, and duplication or sale of all or part of any of the repository collections is not permitted, except that material may be duplicated by you for your research use or educational purposes in electronic or print form. You must obtain permission for any other use. Electronic or print copies may not be offered, whether for sale or otherwise to anyone who is not an authorised user.

Vacancy recovery and vacancy-hydrogen interaction in niobium and tantalum studied by positrons

P. Hautojärvi, H. Huomo, M. Puska, and A. Vehanen

Laboratory of Physics, Helsinki University of Technology, SF-02150 Espoo, Finland

(Received 26 November 1984; revised manuscript received 20 May 1985)

Positron-lifetime measurements in electron-irradiated pure Nb and Ta show that monovacancy migration occurs at 220 and 260 K, respectively. Hydrogen impurities can be bound to vacancies, as is experimentally observed in Ta at 70 K after low-temperature α -particle irradiation. The vacancy-hydrogen complex formation shifts the vacancy migration to higher temperatures. Vacancy-hydrogen complexes retain the capability to trap positrons. Theoretical calculations performed for hydrogen and positron states at vacancies are in agreement with experimental findings.

I. INTRODUCTION

Niobium and tantalum are materials of great importance for high temperature technology and for advanced fission and fusion reactors. However, their defect properties are poorly known because of the strong effects of interstitial impurities, especially hydrogen.¹

Although the melting temperatures of niobium and tantalum are high, the low values of the elastic constants indicate low vacancy migration enthalpies.² Experimental information on vacancy migration has been obtained using different methods, but existing results are still controversial.

Schultz and co-workers^{1,3,4} have shown that the stage III in the resistivity-recovery curve corresponding to vacancy migration in the one-interstitial model¹ occurs in electron-irradiated niobium and tantalum below room temperature at around 220–250 K. This stage is extremely sensitive to various impurities: e.g., the presence of a few ppm of hydrogen can totally remove the stage and a new stage appears above 350 K. On the other hand, the high-temperature results on vacancy formation and self-diffusion energies seem to indicate that vacancy migration in irradiated niobium and tantalum should occur above 480 and 380 K, respectively.⁵

In recent perturbed angular correlation measurements, Sielemann *et al.*⁶ have found defect trapping around 250 K at In(111) probe atoms implanted in niobium. In tantalum Weidinger *et al.*⁷ have found defect trapping at In(111) probes around 360 K, whereas Metzner *et al.*⁸ have observed it already at 250 K. These results have been explained assuming that the migrating defect is a monovacancy.^{6,8} Positron annihilation^{9,10} is known to be a unique and highly defect specific method to follow the evolution of vacancy population in irradiated metals. Positrons get trapped at vacancies and vacancy clusters, which cause large changes in annihilation characteristics, whereas they are insensitive to interstitials and their small agglomerates. Haaf *et al.*¹¹ have found evidence for vacancy migration at 420 K in niobium and at 380 K in tantalum. Our previous results¹² on electron irradiated niobium have shown vacancy migration at 380 K in a sample assumed to contain hydrogen. In neutron irradiated

niobium the vacancy migration within collision cascades was observed already at 160 K independent of the hydrogen content.¹²

In this report, we study electron and α -particle irradiated niobium and tantalum by positron lifetime measurements. The results show that in pure metals vacancy migration and clustering occur below room temperature. Hydrogen atoms can be bound to monovacancies and the vacancy migration is then shifted to higher temperatures. In addition, we perform theoretical calculations, which give information about the hydrogen state at a vacancy and which are in good agreement with our experimental findings on positron trapping at vacancy-hydrogen complexes.

II. EXPERIMENTAL

The samples measuring $6 \times 6 \times 0.04$ mm³ were prepared of high-purity degassed niobium and tantalum foils supplied by H. Schultz from Max-Planck-Institute in Stuttgart. The residual resistivity ratio of the similarly prepared material is between 3000 and 4000. Hydrogen is a common contaminant in these materials. To reduce hydrogen concentration to a ppm level a degassing in ultra-high vacuum for several days is required.¹³

The Nb samples were cut from two different dispatches of nominally pure (< 5 at. ppm H) niobium although their hydrogen content was not checked. A virgin surface can easily pick up hydrogen from the ambient atmosphere, and therefore Nb sample 1 was handled in an He atmosphere. Our results in Sec. III indicate that sample 1 is clean but Nb sample 2 contains a few hundred at. ppm or more hydrogen (see also Ref. 12 and conclusions of the same sample 2 therein). A hydrogen-doped tantalum sample was prepared by annealing a Ta foil in purified H₂ gas at 550 K and then slowly cooled to room temperature. After this treatment, hydrogen concentration was of the order of 5 at. %.¹⁴

The specimens were irradiated with 3 MeV electrons at Centre d'Etudes Nucléaires, Grenoble to a dose of 10^{19} e⁻/cm². During the irradiation under liquid hydrogen the temperature was 21 K and thereafter it was raised to 77 K. Because of the lack of information on low-

temperature resistivity recovery and the Frenkel pair resistivity value, we were not able to estimate the initial defect concentration, but we expected it to be of the order of 100 at. ppm at 77 K. To study the defect recovery below 77 K, we performed α irradiations at 14.7 MeV to a dose of about 2×10^{16} α/cm^2 with the cyclotron of the University of Jyväskylä. During the irradiations the samples were kept under vacuum at 15 K using a closed-loop He cryocooler. The lifetime measurements were performed at 15 K for isochronal annealings between 15 and 200 K. In all experiments the isochronal annealing time was 30 min for 20 K steps to allow as a comparison to other experiments.

Positron-lifetime spectra were measured with a conventional fast-slow coincidence system. The time resolution was 220 psec full width at half maximum (FWHM) (Ref. 15) for electron irradiated samples and 320 psec FWHM for α -irradiated samples. The ^{22}Na positron source with an activity of 10 μCi was evaporated on a thin (1.1 mg/cm²) Ni foil. After source-background subtractions the lifetime spectra were analyzed as a sum of two exponential decay components. From the lifetime values τ_i and their relative intensities I_i we calculated the average positron lifetime $\bar{\tau}$:

$$\bar{\tau} = I_1\tau_1 + I_2\tau_2.$$

This parameter is the statistical mean of the lifetime distribution and it is rather insensitive to uncertainties in the decomposition procedure. Thus it can be used as a sensitive measure for changes in the defect configuration in the sample.¹⁶

III. RESULTS

A. Tantalum

Figure 1 shows some typical positron-lifetime spectra before and after electron irradiation. For the lifetime value of free positions in well-annealed, unirradiated tan-

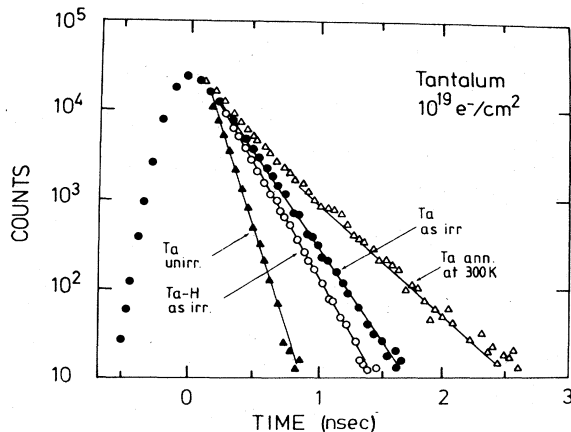


FIG. 1. Examples of the positron lifetime spectra in electron irradiated tantalum. A clear difference between as-irradiated states of pure and hydrogen doped tantalum can be seen. This is due to hydrogen atoms which are mobile below measuring temperature. Further broadening of the spectrum after 300-K annealing corresponds to vacancy clustering.

talium we measure $\tau_f = 120 \pm 2$ psec. The irradiation induced vacancies trap positrons and the lifetime spectra become broader. In the as-irradiated state at 77 K, pure and hydrogen-doped samples show a difference which is attributed to decoration of vacancies by hydrogen atoms. Further broadening of the lifetime spectra occurs after annealing at higher temperatures and in pure tantalum at 300 K an intense long-lifetime component is clearly visible. This component is due to positrons trapped at small three-dimensional vacancy clusters formed during vacancy migration.

Figure 2 shows the behavior of the positron-lifetime parameters in tantalum after electron irradiation as a function of the isochronal annealing temperature. At 77 K the lifetime spectrum is one-exponential with a lifetime value of $\tau_v = 203 \pm 2$ psec. Thus the concentration of irradiation-induced vacancies is sufficiently high to saturate the positron trapping, i.e., all positrons annihilate at vacancies and the lifetime value $\tau_v = 203$ psec is characteristic of monovacancies. At 260 K the average lifetime increases abruptly and the spectrum splits into two components. The longer lifetime τ_2 varies between 340 and 420 psec with the intensity $I_2 = 50-60\%$. This is a clear indication of vacancy migration and clustering. The τ_2 component is due to positron trapping at small three-dimensional vacancy cluster, which is known to be the only defect configuration giving such a long lifetime.^{17,18} From the measured τ_2 values we can estimate^{17,18} that the

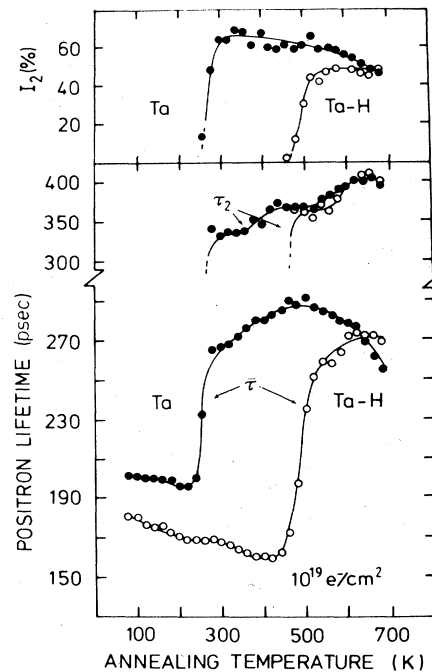


FIG. 2. Average positron lifetime $\bar{\tau} = I_1\tau_1 + I_2\tau_2$ and the longer lifetime component τ_2, I_2 in electron-irradiated Ta as a function of annealing temperature. The increase of $\bar{\tau}$ and the appearance of the τ_2 component shows the vacancy migration and clustering at 260 K in pure Ta. The vacancies in Ta-H are blocked by hydrogen atoms and vacancy clustering is shifted to 450 K.

size of the vacancy clusters varies from 5 to 20 monovacancies. These clusters seem to be very stable since they persist above 700 K annealing.

The hydrogen doping has no effect of the free positron lifetime in unirradiated tantalum. However, after electron irradiation the positron lifetime at 77 K is only 180 ± 2 psec. This is well below the value of $\tau_v = 203$ psec in the pure sample, although the lifetime spectrum is again one-exponential showing saturation trapping. The difference is evidently due to hydrogen atoms, which are mobile already at low temperatures and able to decorate the irradiation-induced vacancies at around 70 K, as will be discussed below. Due to hydrogen decoration the free volume of a vacancy is reduced, the electron density is higher and thus a trapped positron annihilates faster. The lifetime value of $\tau_{v-H} = 180$ psec is attributed to a monovacancy decorated by one or two hydrogen atoms (see Sec. IV). During annealing between 77–400 K the lifetime of trapped positrons shows a continuous decrease perhaps due to further decoration or relaxation of the vacancy-hydrogen complexes. No evidence of vacancy migration is seen at 260 K, and the formation of the longer lifetime component τ_2 and the increase of the average lifetime $\bar{\tau}$ is shifted above 450 K. Again the component $\tau_2 = 350$ –420 psec with $I_2 \approx 50\%$ can be assigned to positron trapping at small three-dimensional vacancy clusters. The clusters seem to be stable at least up to the maximum annealing temperature of 700 K.

The reason for the differences between pure and hydrogen-doped specimens is evident: vacancies are blocked by hydrogen atoms and vacancy clustering cannot occur until around 480 K where the dissociation of the vacancy-hydrogen complexes occur or the complexes start to migrate.

The trapping of hydrogen at vacancies was studied by irradiating tantalum samples with 14.7 MeV α particles at 15 K. Figure 3 shows the average lifetime $\bar{\tau}$ during annealing of pure and hydrogen-doped tantalum. After irradiation there is no saturation in positron trapping, since the depth profile of irradiation-induced defects does not

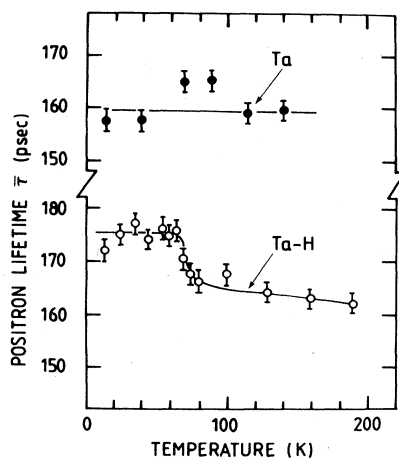


FIG. 3. Recovery of the average positron lifetime $\bar{\tau}$ in α -irradiated Ta. Hydrogen trapping at irradiation-induced vacancies is seen as a small drop of $\bar{\tau}$ between 60–70 K in Ta-H.

completely overlap with the positron implantation profile, and a fraction of positrons always annihilates in an undamaged part of the sample. The different levels of $\bar{\tau}$ in the two samples reflect slightly different irradiation doses. In the pure sample the lifetime spectrum stays constant indicating no observable recovery of vacancy type defects below 200 K. However, a drop of about 10 psec starting at 60 K in hydrogen-doped tantalum is observed. This occurs at the same temperature where Schultz and co-workers^{1,19} have seen a hydrogen associated peak in the resistivity recovery of electron irradiated tantalum. We attribute the drop in $\bar{\tau}$ to the decoration of vacancies by hydrogen atoms. Although our sample contains several atomic percent of hydrogen all of it is expected to be immobile in the ordered β phase at low temperatures.¹⁴ The results of Hanada *et al.*²⁰ show that the concentration of freely migrating hydrogen in solid solution α phase increases rapidly from 1 to 50 at. ppm between 60 and 80 K. This hydrogen concentration is roughly similar to the irradiation-induced vacancy concentration in our sample and therefore free hydrogen atoms are able to decorate a significant fraction of vacancies. In fact, an unconstrained two-component fit below 60 K shows a lifetime $\tau_2 = 200 \pm 20$ psec with an intensity $I_2 \approx 60\%$. This component is evidently due to undecorated vacancies and it cannot be resolved above 80 K. The vacancy clustering demonstrated by the formation of a lifetime component of about 350 psec is observed (but not shown in Fig. 3) at 250 and 450 K in α -irradiated pure and hydrogen-doped tantalum, respectively. These recovery temperatures are similar to electron irradiated samples and thus we can conclude that we do not observe any changes in He-defect complexes between 15–500 K temperatures.

B. Niobium

The lifetime of free positrons in well-annealed niobium is measured to be $\tau_f = 122 \pm 2$ psec. The behavior of the lifetime parameters after electron irradiation for two different specimens are shown in Fig. 4. The results of sample 2 have been discussed also earlier.¹² In the case of sample 1 much care has been taken to avoid hydrogen contamination. We think that the results for sample 1 are representative of pure niobium. Again the irradiation increases the lifetime to $\tau_v = 210 \pm 2$ psec. The spectrum is single-exponential indicating that all positrons annihilate while trapped at monovacancies. The splitting into two lifetime components due to formation of vacancy clusters occurs now at 220 K during vacancy migration. The lifetime τ_2 is about 400 psec with $I_2 \approx 30\%$. However, I_2 and τ_2 start to decrease already below 300 K showing the dissolution or collapse of the small three-dimensional vacancy clusters.

The results of niobium sample 2 show remarkable differences. The lifetime value at 77 K after irradiation is only 170 ± 2 psec and less than τ_v , although the spectra indicate saturation trapping. The splitting into two components due to vacancy cluster formation is shifted to 380 K. These differences are similar to those found between pure and hydrogen-doped tantalum. This gives strong support to the idea presented previously that sample 2

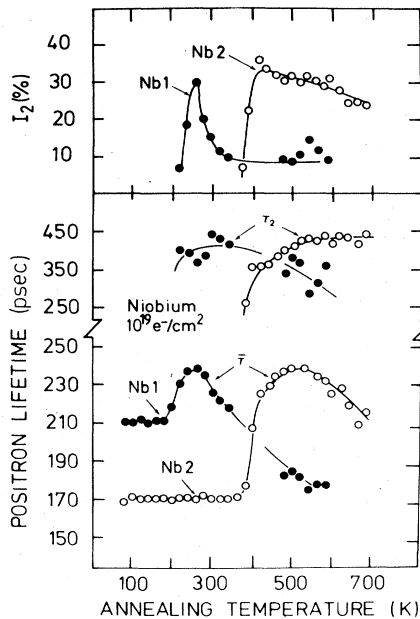


FIG. 4. Average positron lifetime $\bar{\tau}=I_1\tau_1+I_2\tau_2$ and the longer lifetime component τ_2, I_2 in electron-irradiated Nb as a function of annealing temperature. The increase of $\bar{\tau}$ and the appearance of the τ_2 component at 220 K in sample 1 is attributed to vacancy migration and clustering in pure Nb. In sample 2 the vacancy clustering is shifted to 380 K due to hydrogen impurities.

contains a sufficient amount of hydrogen impurities (100 at. ppm or more) to decorate the irradiation-induced vacancies (for more detailed discussion see Ref. 12). Vacancy migration is blocked until the dissociation of the vacancy-hydrogen complexes occurs at 380 K. It is also interesting to note that the vacancy clusters in sample 2 are much more stable, surviving up to 700 K. This indicates that hydrogen has an important role in stabilizing the small three-dimensional vacancy clusters. Similar behavior has also been observed in neutron irradiated niobium.¹²

IV. HYDROGEN AND POSITRON STATES AT VACANCIES

We have calculated the hydrogen state in niobium and tantalum vacancies by using the effective medium theory²¹ and then estimated the corresponding positron annihilation characteristics by applying the computational scheme of Puska and Nieminen.¹⁸ In our effective medium calculations the potential for hydrogen at a given point r is assumed to depend via a universal functional²¹ $E_{\text{hom}}(n)$ on the average electron density $n(r)$ seen by the hydrogen atom around r . The sampled density n is calculated by superposition of free atoms. The potential is inserted in the full three-dimensional Schrödinger equation for the hydrogen mass coordinate and the wave function is solved by numerical relaxation techniques.²² The result for hydrogen trapped in a niobium vacancy is shown in

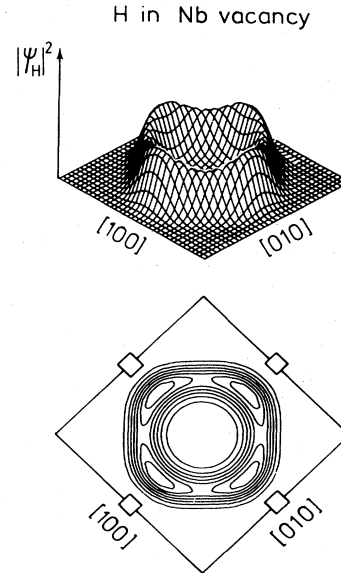


FIG. 5. Ground-state hydrogen density at a Nb vacancy. The density is shown on a (100) plane and the octahedral sites adjacent to the vacancy are denoted by open squares. The contour spacing is one-tenth of the maximum value.

Fig. 5. As can be seen, the hydrogen wave function is delocalized over the entire vacancy with maxima between the vacancy center and the six adjacent octahedral sites. The maxima are at a distance of $0.3a$ (a is the lattice constant) from the vacancy center. In tantalum, the maxima are less pronounced and their distance from the vacancy center is only $0.15a$.

The calculation of the positron state can utilize the fact that due to its light mass, the trapped positron is able to follow adiabatically the motion of the hydrogen atom in the vacancy.²³ However, for simplicity, in the positron state calculations the hydrogen atom is fixed at the position of its maximum density, at a distance of $0.3a$ in niobium and $0.15a$ in tantalum from the vacancy center toward an octahedral site. The potential for the positron is constructed¹⁸ by superimposing free-atom Coulombic potentials and introducing a correlation part in a local approximation by using superimposed electron densities and electron-gas data for the correlation energy. The calculation¹⁸ of the positron lifetime also employs superimposed atomic electron densities. The enhancement effects of the annihilation rate are handled by using the Brandt-Reinheimer formula for the valence electron contribution, in which also the hydrogen-induced electron is included. A constant enhancement factor of 1.5 for tightly bound core electrons and a constant enhancement factor γ_d for the outermost rather polarizable d -level electrons are used. γ_d is fitted so that the calculation for the perfect lattice agrees with the experimental free positron lifetime in a well-annealed metal sample. For niobium we find $\gamma_d=3.26$ and for tantalum $\gamma_d=2.89$.

The results for positron lifetimes and binding energies are shown in Table I. First we see that the calculated lifetimes for positrons trapped at pure monovacancies agree

TABLE I. Calculated lifetimes τ^{theor} and binding energies E_B^{theor} for positrons trapped at a monovacancy or vacancy-hydrogen complexes.

	Niobium			Tantalum		
	τ^{theor} (psec)	τ^{expt} (psec)	E_B^{theor} (eV)	τ^{theor} (psec)	τ^{expt} (psec)	E_B^{theor} (eV)
bulk	120	120±2		120	120±2	
vac	216	210±2	3.2	222	203±2	8.7
vac-1H	192	170±2	2.7	182	180±2	7.6
vac-2H	167			155	160±2	

well with the measured values. Theoretical values tend to be slightly larger than the experimental ones, which is most probably a consequence of the lattice relaxation ignored in the calculations. The positron-vacancy binding energy E_B , which is measured from the ground-state energy level of a delocalized positron, is found to be 3.2 eV in niobium and 8.7 eV in tantalum. The much higher value of E_B in tantalum originates from the higher energy of the delocalized positron state. The lattice parameters are about the same in both metals ($a=3.30$ Å), but because of the bigger size of atoms, a positron feels much stronger Coulombic repulsion in tantalum than in niobium. Gupta and Siegel²⁴ have reported positron-vacancy binding energies of 4.6 and 4.9 eV for niobium and tantalum, respectively. These values, based on augmented-plane-wave (APW) supercell calculations, are intermediate compared to the present ones.

Our results indicate that positron detrapping from thermally generated vacancies is not possible in tantalum, but may be non-negligible in niobium.²⁵ Detrapping was taken into account both in tantalum and niobium by Maier *et al.*⁵ in analyzing their high-temperature experiments. This procedure has a tendency to underestimate vacancy formation enthalpies and thus to overestimate vacancy migration enthalpies.

The introduction of one hydrogen atom at a vacant site at the position of its maximum density decreases the positron binding energy by 0.5–1 eV, but does not suppress the positron trapping. As a matter of fact, the strong electron charge transfer toward a proton occurring in a free-electron-like environment can even increase the positron binding energy relative to the pure vacancy.²¹ The trapped positron lifetime decreases from 216 to 192 psec in niobium and from 222 to 182 psec in tantalum due to one hydrogen atom fixed at a distance of $0.3a$ and $0.15a$ from the vacancy center, respectively. These values are, however, not very sensitive to the hydrogen position. A hydrogen atom placed at the center of a vacancy would result in lifetimes of 172 and 175 psec in niobium and tantalum, respectively.

The introduction of a second hydrogen atom on the opposite side of the vacancy, at the same distance from the center ($0.3a$ in Nb and $0.15a$ in Ta), further decreases the positron lifetime to 167 psec in niobium and to 155 psec in tantalum. However, the calculated positron binding energies do not change much showing that positrons can be trapped at a vacancy containing even two hydrogen atoms.

The experimental lifetime values for positrons at hydrogen-decorated vacancies are between the calculated values for a vacancy-hydrogen pair and a vacancy–two-hydrogen complexes. It is interesting to see from Fig. 2 that in hydrogen-doped tantalum, where the hydrogen concentration is much bigger than the number of vacancies, the trapped positron lifetime decreases from 180 psec at 77 K to 160 psec at 420 K probably due to further decoration of vacancy-hydrogen pairs or complexes during annealing.

In conclusion, the calculations give firm evidence that positron trapping does occur at hydrogen decorated vacancies. The estimated lifetimes for trapped positrons at vacancies containing one or two hydrogen atoms agree well with the experimental values in irradiated niobium and tantalum samples containing hydrogen.

V. DISCUSSION AND CONCLUSIONS

Our experiments show clearly that the migration of vacancies in pure niobium and tantalum occurs below room temperature. The results also demonstrate that hydrogen trapping at vacancies around 70 K causes a shift in vacancy migration to higher temperatures. These findings are in perfect agreement with the observations on the stage III recovery of electrical resistivity in niobium and tantalum made by Schultz and co-workers.^{1,3,4} Also, recent perturbed angular-correlation experiments^{6,8} can be consistently explained when the defects found to migrate in these metals between 200 and 300 K are vacancies. The vacancy migration at 220–260 K indicates that the migration enthalpy is about 0.6–0.7 eV, and recent quenching experiments²⁶ report values of 0.6–0.9 eV for niobium and 0.7 eV for tantalum. Other experiments indicating vacancy migration above room temperature^{7,11} are most likely explained by a small amount of hydrogen in the specimens.

From the results for samples with hydrogen impurities we can estimate an upper limit to the vacancy-hydrogen binding energy. The disappearance of vacancy-hydrogen complexes at 380 K in niobium and at 450 K in tantalum corresponds to a dissociation energy of about 1.1 and 1.3 eV, respectively. If we assume that only a single hydrogen is bound at a vacancy then the dissociation energy is the sum of the binding energy and the migration energy of the faster moving constituent; i.e., that of hydrogen. The migration energy of hydrogen in both metals is about 0.1

eV,²⁷ and thus values of 1.0–1.2 eV for the vacancy-hydrogen binding energy are obtained. These are rather high, but within the limits proposed for vacancy-hydrogen binding energies in metal.²⁸

Our theoretical calculations confirm well the experimental observations on positron and hydrogen interactions with vacancies. The hydrogen trapped in a vacancy is partly delocalized over the entire vacancy having, however, maximum densities outside the center close to the adjacent octahedral sites. This off-center structure of vacancy-hydrogen pairs in some fcc and bcc metals has been seen by channeling experiments²⁸ and evidence even for the delocalized state of trapped deuterium in nickel vacancy has recently been reported.²⁹ Positrons can be trapped at vacancies decorated by one or two hydrogen atoms and the calculated annihilation characteristics are in agreement with positron lifetime measurements.

Our results on niobium and tantalum together with the previous ones on α -iron¹⁶ verify the early idea² that in spite of their high melting temperature the vacancy migration temperature and enthalpy in some bcc metals may be surprisingly low because of the low values of the elastic constants.

ACKNOWLEDGMENTS

The authors are grateful to Professor H. Schultz for the sample material and helpful discussions. We are also indebted to Dr. P. Moser and the Section de Accélérateurs de Centre d'Etudes Nucléaires, Grenoble, for electron irradiations, as well as to R. Talja and H. Rajainmäki from University of Jyväskylä for α irradiations. The contribution of F. Plazaola in the positron experiments is gratefully acknowledged.

¹For references see H. Schultz, in *Point Defects and Defect Interactions in Metals*, edited by J.-I. Takamura, M. Doyama, and M. Kiritani (University of Tokyo Press, Tokyo, 1982), p. 183.

²H. Schultz, *Scr. Metall.* **8**, 721 (1974).

³K. Faber and H. Schultz, *Rad. Eff.* **31**, 157 (1977).

⁴H. Kugler, I. A. Schwirlich, S. Takaki, K. Yamakawa, U. Ziebart, J. Petzold, and H. Schultz, in *Point Defects and Defect Interactions in Metals*, Ref. 1, p. 520.

⁵K. Maier, M. Peo, B. Saile, H. E. Schäfer, and A. Seeger, *Philos. Mag. A* **40**, 701 (1979).

⁶R. Sielemann, H. Metzner, R. Butt, S. Klaumünzer, H. Haas, and G. Vogl, *Phys. Rev. B* **25**, 5555 (1982).

⁷A. Weidinger, M. Deicher, and J. Busse, in *Point Defects and Defect Interaction in Metals*, Ref. 1, p. 268.

⁸H. Metzner, R. Sielemann, R. Butt, S. Klaumünzer, and W. Semmler, *Hyperfine Interact.* **15/16**, 413 (1983).

⁹*Positrons in Solids*, Vol. 12 of *Topics in Current Physics*, edited by P. Hautojärvi (Springer, Heidelberg, 1979).

¹⁰*Positron Solid State Physics*, Proceedings of the International School of Physics "Enrico Fermi," Course No. 83, edited by W. Brandt and A. Dupasquier (North-Holland, Amsterdam, 1983).

¹¹M. Haaf, H.-E. Schäfer, and W. Frank, in *Proceedings of the 6th International Conference on Positron Annihilation*, edited by P. G. Coleman, S. C. Sharma, and L. M. Diana (North-Holland, Amsterdam, 1982), p. 446.

¹²P. Hautojärvi, H. Huomo, P. Saariaho, A. Vehanen, and J. Yli-Kaupilla, *J. Phys. F* **13**, 1415 (1983).

¹³K. Faber, J. Shweikhardt, and H. Schultz, *Scr. Metall.* **8**, 713 (1974).

¹⁴T. Schrober and H. Wenzl, in *Hydrogen in Metals*, Vol. 29 of *Topics in Current Physics*, edited by G. Alefeld and J. Völkl

(Springer, Berlin, 1978), p. 11.

¹⁵K. Rytsölä, *Nucl. Instrum. Methods* **199**, 491 (1982).

¹⁶A. Vehanen, P. Hautojärvi, J. Johansson, J. Yli-Kaupilla, and P. Moser, *Phys. Rev. B* **25**, 762 (1982).

¹⁷P. Hautojärvi, J. Heiniö, M. Manninen, and R. Nieminen, *Philos. Mag.* **35**, 973 (1977).

¹⁸M. J. Puska and R. M. Nieminen, *J. Phys. F* **13**, 333 (1983).

¹⁹H. Kugler, I. A. Schwirlich, S. Takaki, U. Ziebart, and H. Schultz, in *Point Defects and Defect Interactions in Metals*, Ref. 1, p. 191.

²⁰R. Hanada, T. Sukanuma, and H. Kimura, *Scr. Metall.* **6**, 483 (1972).

²¹J. K. Nørskov and N. D. Lang, *Phys. Rev. B* **21**, 2316 (1980); M. J. Stott and E. Zaremba, *ibid.* **22**, 1564 (1980); for the most recent development, see P. Nordlander, S. Holloway, and J. K. Nørskov, *Surf. Sci.* **136**, 591 (1984).

²²M. J. Puska and R. M. Nieminen, *Phys. Rev. B* **29**, 5382 (1984).

²³H. E. Hansen, R. M. Nieminen, and M. J. Puska, *J. Phys. F* **14**, 1299 (1984); P. Jena, M. J. Ponnambalam, and M. Manninen, *Phys. Rev. B* **24**, 2884 (1981).

²⁴R. P. Gupta and R. W. Siegel, *J. Phys. F* **10**, L7 (1980).

²⁵M. Manninen and R. M. Nieminen, *Appl. Phys. A* **26**, 93 (1981).

²⁶M. Tietze, S. Takaki, I. A. Schwirlich, and H. Schultz, in *Point Defects and Defect Interactions in Metals*, Ref. 1, p. 265.

²⁷J. Völkl and G. Alefeld, in *Hydrogen in Metals*, Vol. 28 of *Topics in Current Physics*, edited by G. Alefeld and J. Völkl (Springer, Berlin, 1978), p. 321.

²⁸S. T. Picraux, *Nucl. Instrum. Methods* **182/183**, 413 (1981).

²⁹F. Besenbacher, H. Bøgh, A. A. Pisarev, M. J. Puska, S. Holloway, and J. K. Nørskov, *Nucl. Instrum. Methods B* **4**, 374 (1984).